C

LBL-8846 c.2
Preprint

Lawrence Berkeley Laboratory

UNIVERSITY OF CALIFORNIA

ENERGY & ENVIRONMENT DIVISION

Submitted to the Journal of Chemical Physics

VALENCE BOND MODEL POTENTIAL ENERGY SURFACE FOR H_4

David M. Silver and Nancy J. Brown

February 1979

RECEIVED
LAWRENCE
BERKELEY LABORATORY

OCT 15 1979

LIBRARY AND
DOCUMENTS SECTION

TWO-WEEK LOAN COPY

This is a Library Circulating Copy which may be borrowed for two weeks. For a personal retention copy, call Tech. Info. Division, Ext. 6782

Prepared for the U.S. Department of Energy under Contract W-7405-ENG-48

LBL-8846 c.2

DISCLAIMER

This document was prepared as an account of work sponsored by the United States Government. While this document is believed to contain correct information, neither the United States Government nor any agency thereof, nor the Regents of the University of California, nor any of their employees, makes any warranty, express or implied, or assumes any legal responsibility for the accuracy, completeness, or usefulness of any information, apparatus, product, or process disclosed, or represents that its use would not infringe privately owned rights. Reference herein to any specific commercial product, process, or service by its trade name, trademark, manufacturer, or otherwise, does not necessarily constitute or imply its endorsement, recommendation, or favoring by the United States Government or any agency thereof, or the Regents of the University of California. The views and opinions of authors expressed herein do not necessarily state or reflect those of the United States Government or any agency thereof or the Regents of the University of California.

Valence Bond Model Potential Energy Surface for H_4

David M. Silver
Applied Physics Laboratory
The Johns Hopkins University
Laurel, Maryland 20810

and

Nancy J. Brown
Energy and Environment Division
Lawrence Berkeley Laboratory
University of California
Berkeley, California 94720

This work was supported in part by the Department of the Navy, Naval Sea Systems Command, under Contract N00024-78-C-5384 at The Johns Hopkins University Applied Physics Laboratory, and in part by the Office of Energy Research, Basic Energy Sciences Division of the Department of Energy under Contract No. W-7405-ENG-48 at the Lawrence Berkeley Laboratory Energy and Environment Division.

ABSTRACT

Potential energy surfaces for the H_4 system are derived using the valence bond procedure. An *ab initio* evaluation of the valence bond energy expression is described and some of its numerical properties are given. Next, four semi-empirical evaluations of the valence bond energy are defined and parameterized to yield reasonable agreement with various *ab initio* calculations of H_4 energies. Characteristics of these four H_4 surfaces are described by means of tabulated energy minima and equipotential countour maps for selected geometrical arrangements of the four nuclei.

I. Introduction

The bimolecular hydrogen-deuterium chemical exchange reaction, $H_2 + D_2 \rightarrow 2\ HD$, depends on the motions of the constituent four electrons and four nuclei of the system. By invoking the Born-Oppenheimer approximation[1], a separation of electronic and nuclear motions is achieved whereby, for any given fixed set of nuclear positions, a four-electron Schrodinger equation is defined. The energy eigenvalue of this equation together with the nuclear-nuclear repulsion terms forms a potential field which governs the motion of the nuclei. This interaction potential, being dependent on the geometrical positions of the four nuclei, is a function of six inter-nuclear distances. The development of a suitable mathematical form for this interaction potential is a necessary precursor to an application of scattering theory to the dynamical aspects of the overall chemical reaction.

Calculations have been performed[2-13] on the H_4 system using various *ab initio* methods. In principle, these calculations are capable of giving accurate estimates of barrier heights and other properties of the system. However, since high quality quantum mechanical descriptions entail a large computational effort, there is a limit to these pursuits. Thus the existing *ab initio* calculations have been necessarily limited to an examination of highly symmetric geometries of the full six-dimensional potential surface.

In order to be particularly useful for a study of reaction dynamics, it is necessary that the value of the interaction potential be rapidly available for any arbitrary conformation of the nuclei. In addition, trajectory calculations

require the partial derivatives of the potential with respect to each of the internuclear coordinates. The surface must have proper asymptotic and limiting behavior, such as the dissociation into four atoms, equilibrium separations and binding energies for the diatomic components of the system, and removal of one atom to form H_3. In addition, it is desired that the magnitude and position of various reaction barriers be in reasonable agreement with ab initio calculations of these quantities.

One approach would be to choose a convenient mathematical form for the potential and fit it to some of the available ab initio values. Although reasonable agreement would be insured for the fitted values, the quality of the potential in the remainder of the six-dimensional space would be largely unknown. Instead, a simple model wavefunction can be chosen to represent the system and semi-empirical methods can be invoked for the evaluation of electron repulsion integrals. This type of potential surface can be parameterized to give agreement with some ab initio results; and in the remainder of the six-dimensional space, the potential would have properties governed by the nature of the model wavefunction and the approximations used for electron repulsion integrals. Previous semi-empirical approaches[14-21] have introduced the further approximation that all overlap integrals are set to zero, which has led to poor agreement with ab initio results, especially for the magnitude of the lowest barrier for chemical exchange.

The present work employs the valence bond theory to generate a simple model wavefunction. The potential surface is constructed using the semi-empirical treatment of the London-Eyring-Polanyi-Sato type[22-24], but modified to include all overlap and multiple exchange integrals. This is a generalization to four atoms of the procedure developed previously by Porter and Karplus[25] for the H_3 potential surface, which has found utility in

studying the hydrogen atom-molecule, $H + H_2$, exchange process[26]. Various *ab initio* results[10,13] are used to parameterize the present H_4 surface and, in addition, the previous[25] H_3 parameterization is incorporated. Hence, when one atom is separated by a large distance from the other three, the H_4 surface reduces exactly to the previous[25] Porter-Karplus H_3 surface.

An alternative parameterization scheme could be envisioned in which the potential surface is tailored to agree with the results of shock tube studies[27,28] of the $H_2 + D_2$ system. The experimental results have been shown[27-30] to be consistent with a mechanism requiring vibrational excitation of the reactant species and an activation energy of about 40 kcal/mole. However, objections have been raised[31] concerning the interpretation of the experimental results[27] and qualitative molecular orbital arguments have been given[32] which suggest that a much higher activation energy should be expected. Although there are discrepancies between *ab initio* and experimental results on the short-range interaction between two hydrogen molecules, the *ab initio* results[4,7-13] have been shown[33] to be quite consistent with one another. Moreover, reasonable agreement has been found between *ab initio* results[12,13] and molecular beam measurements[34] for the long-range interactions. Therefore, the parameterization of the potential surface has been chosen to give agreement exclusively with *ab initio* results.

The valence bond formulation of the potential surface is described in Section II. The quality of the simple valence bond procedure is assessed in Section III by comparing valence bond and configuration interaction calculations on H_4 using exact evaluations of all electron repulsion integrals (*ab initio*). The semi-empirical approximations are described in Section IV and the properties of the corresponding potential surfaces are presented in Section V. A short discussion follows.

II. Valence Bond Formulation

The details of the non-ionic valence bond treatment for the four orbital, four-electron H_4 system have been given[35] and therefore only the pertinent results are presented here. The four nuclei are designated A, B, C and D. The basis set consists of a hydrogenic 1s orbital on each of these centers, correspondingly labelled a, b, c and d.

The valence bond wavefunction, Ψ_{VB}, is constructed from two linearly independent canonical structures, Ψ_I and Ψ_{II},

$$\Psi_{VB} = A_I \psi_I + A_{II} \psi_{II} \tag{1}$$

corresponding to the bonding arrangements (A-B, C-D) and (A-D, B-C), respectively. The relative weights of these component structures is found by solving a set of secular equations involving the Hamiltonian

$$\mathcal{H} = -\tfrac{1}{2} \sum_{p=1} \nabla_p^2 - \sum_{p\alpha} r_{p\alpha}^{-1} + \sum_{p<q} r_{pq}^{-1} + \sum_{\alpha<\beta} R_{\alpha\beta}^{-1} \tag{2}$$

where p, q refer to electrons, and α, β refer to nuclei. The lowest eigenvalue, E_{VB}, can be written as follows:

$$E_{VB} = [f_1 - (f_1^2 - f_2 f_3)^{\frac{1}{2}}]/f_3 \tag{3}$$

where the functions f are defined in terms of matrix elements of $\mathcal{H}$ and overlap integrals with respect to ψ_I and ψ_{II}:

$$f_1 = \tfrac{1}{2}\langle I|\mathcal{H}|I\rangle\langle II|II\rangle + \tfrac{1}{2}\langle II|\mathcal{H}|II\rangle\langle I|I\rangle - \langle I|\mathcal{H}|II\rangle\langle I|II\rangle \tag{4}$$

$$f_2 = \langle I|\mathcal{H}|I\rangle\langle II|\mathcal{H}|II\rangle - \langle I|\mathcal{H}|II\rangle^2 \tag{5}$$

$$f_3 = \langle I|I\rangle\langle II|II\rangle - \langle I|II\rangle^2 \tag{6}$$

A. Matrix elements of $\mathcal{H}$

Explicit expressions for the matrix elements of $\mathcal{H}$ in Eqs. (4) - (6) can be written as follows:

$$\langle I|\mathcal{H}|I\rangle = 2[2Q + 3({}^1J_1 + {}^1J_6) - {}^1J - 2^2J + 2(-{}^3J_{146} - {}^3J_{156} + 2\,{}^3J_{245})] \tag{7}$$

$$\langle II|\mathcal{H}|II\rangle = 2[2Q + 3({}^1J_3 + {}^1J_4) - {}^1J - 2^2J + 2(-{}^3J_{146} + 2\,{}^3J_{156} - {}^3J_{245})] \tag{8}$$

$$\langle I|\mathcal{H}|II\rangle = 2[-Q + 3({}^1J_2 + {}^1J_5) - {}^1J + {}^2J + 2(2\,{}^3J_{146} - {}^3J_{156} - {}^3J_{245})] \tag{9}$$

The definitions of the symbols used in these expressions are given below.

The Coulomb integral, Q, involves no electron exchanges between the four orbitals and can be decomposed into a sum of diatomic components, Q_i:

$$Q = \langle abcd|\mathcal{H}|abcd\rangle = \sum_{i=1}^{6} Q_i \tag{10}$$

where the numerical subscripts, i, designate either orbital interactions or internuclear distances as appropriate:

1 → ab or AB	2 → ac or AC	3 → ad or AD	
4 → bc or BC	5 → bd or BD	6 → cd or CD	(11)

The diatomic Coulomb terms are defined as follows

$$Q_1 \equiv Q_{ab} = \langle ab|ab\rangle - 2\langle a|r_B^{-1}|a\rangle + R_{AB}^{-1} \tag{12}$$

using the standard integral notations,

$$\langle ab|cd\rangle = \int d\tau_1 \int d\tau_2 \; a(1)b(2)\; r_{12}^{-1}\; c(1)d(2) \tag{13}$$

$$\langle a|\hat{O}|b\rangle = \int d\tau_1 \; a(1)\hat{O}(1)b(1) \quad . \tag{14}$$

The single-exchange integral, ${}^1J_1$, involves a single permutation of two orbitals, for example,

$${}^1J_1 \equiv {}^1J_{ab} = \langle abcd|\mathcal{K}|bacd\rangle \quad . \tag{15}$$

This integral can be decomposed into the following components:

$${}^1J_{ab} = J_{ab} + \Delta_{ab} + Q_{cd}\, S_{ab}^2 \tag{16}$$

where the subscript on Q always corresponds to the two remaining orbitals not involved in the permutation. The diatomic exchange integral has the form

$$J_1 \equiv J_{ab} = \langle ab|ba\rangle - 2\langle a|r_B^{-1}|b\rangle S_{ab} + S_{ab}^2\, R_{AB}^{-1} \;, \tag{17}$$

involving the diatomic overlap integral

$$S_{ab} = \langle a|b\rangle \quad . \tag{18}$$

The remaining term in Eq. (16) consists of a sum of diatomic and triatomic components

$$\Delta_{ab} = S_{ab}^2[R_{AC}^{-1} + R_{BC}^{-1} - \langle c|r_A^{-1} + r_B^{-1}|c\rangle] + 2S_{ab}[\langle ac|bc\rangle - \langle a|r_C^{-1}|b\rangle]$$

$$+ S_{ab}^2[R_{AD}^{-1} + R_{BD}^{-1} - \langle d|r_A^{-1} + r_B^{-1}|d\rangle] + 2S_{ab}[\langle ad|bd\rangle - \langle a|r_D^{-1}|b\rangle] \ . \quad (19)$$

The remaining single-exchange term, ${}^1J$ in Eqs. (7)-(9), is a sum of single-exchange integrals:

$${}^1J = \sum_{i=1}^{6} {}^1J_i \ . \quad (20)$$

The double-exchange term, ${}^2J$ of Eqs. (7)-(9), is a sum of double-exchange integrals of two types:

$${}^2J = ({}^2J_{12} + {}^2J_{15} + {}^2J_{36} + {}^2J_{46}) - ({}^2J_{16} + {}^2J_{25} + {}^2J_{34}). \quad (21)$$

The integrals ${}^2J_{ij}$ in the first set of parentheses involve two permutations i, j of pairs of orbitals, where there is a common orbital in the two pairs; for example,

$${}^2J_{12} \equiv {}^2J_{ab,ac} = \langle abcd|\mathcal{H}|bcad\rangle \ . \quad (22)$$

These integrals involve only three orbitals and can therefore be written in terms of the species,

$${}^2J_{12} = J_{abc} + \Delta_{abc} \quad (23)$$

where J_{abc} contains strictly triatomic components,

$$J_{abc} = S_{ab}\, S_{bc}\, S_{ca}\, (R_{AB}^{-1} + R_{BC}^{-1} + R_{CA}^{-1})$$

$$+ S_{ab}(\langle ac|cb\rangle - \tfrac{1}{2} S_{bc}\langle a|r_B^{-1}+r_C^{-1}|c\rangle - \tfrac{1}{2} S_{ac}\langle b|r_A^{-1}+r_C^{-1}|c\rangle)$$

$$+ S_{bc}(\langle ba|ac\rangle - \tfrac{1}{2} S_{ab}\langle a|r_A^{-1}+r_B^{-1}|c\rangle - \tfrac{1}{2} S_{ac}\langle a|r_A^{-1}+r_C^{-1}|b\rangle)$$

$$+ S_{ac}(\langle ab|bc\rangle - \tfrac{1}{2} S_{bc}\langle a|r_B^{-1}+r_C^{-1}|b\rangle - \tfrac{1}{2} S_{ab}\langle b|r_A^{-1}+r_B^{-1}|c\rangle), \tag{24}$$

and Δ_{abc} contains triatomic interactions with the fourth center,

$$\begin{aligned}\Delta_{abc} = {} & S_{ab}\, S_{bc}\, S_{ac}(R_{AD}^{-1} + R_{BD}^{-1} + R_{CD}^{-1} - \langle d|r_A^{-1} + r_B^{-1} + r_C^{-1}|d\rangle) \\ & + S_{ab}S_{bc}(\langle ad|cd\rangle - \langle a|r_D^{-1}|c\rangle) \\ & + S_{bc}S_{ac}(\langle ad|bd\rangle - \langle a|r_D^{-1}|b\rangle) \\ & + S_{ab}S_{ac}(\langle bd|cd\rangle - \langle b|r_D^{-1}|c\rangle) \quad .\end{aligned} \tag{25}$$

The integrals, ${}^2J_{ij}$, in the second set of parentheses of Eq. (21) involve two permutations i,j of pairs of orbitals, where there is no common orbital in the two pairs; for example,

$${}^2J_{16} \equiv {}^2J_{ab,cd} = \langle abcd|\mathcal{H}|badc\rangle \quad . \tag{26}$$

These integrals have the decomposition,

$${}^2J_{16} = J_{ab}\, S_{cd}^2 + J_{cd}\, S_{ab}^2 + \Delta_{ab,cd}\ , \tag{27}$$

involving the diatomic exchange integral of Eq. (17) and the four-center species

$$\begin{aligned}\Delta_{ab,cd} = {} & S_{ab}^2\, S_{cd}^2(R_{AC}^{-1} + R_{AD}^{-1} + R_{BC}^{-1} + R_{BD}^{-1}) \\ & + 4\, S_{ab}S_{cd}(\langle ac|bd\rangle - \tfrac{1}{2} S_{cd}\langle a|r_C^{-1}+r_D^{-1}|b\rangle - \tfrac{1}{2} S_{ab}\langle c|r_A^{-1}+r_B^{-1}|d\rangle)\end{aligned} \tag{28}$$

The triple-exchange integrals, ${}^3J_{ijk}$ of Eqs. (7)-(9), involve three cyclic permutations i, j, k of pairs of orbitals:

$$J_{146} \equiv J_{ab,bc,cd} = \langle abcd|\mathcal{H}|dabc\rangle \equiv J_{abcd} \tag{29}$$

$$J_{156} \equiv J_{ab,bd,dc} = \langle abcd|\mathcal{H}|cadb\rangle \equiv J_{abdc} \tag{30}$$

$$J_{245} \equiv J_{ac,cb,bd} = \langle abcd|\mathcal{H}|dcab\rangle \equiv J_{acbd} \tag{31}$$

These integrals decompose into triatomic and four-center species:

$$\begin{aligned}
J_{abcd} = {} & S_{ab}\, S_{bc}\, S_{cd}\, S_{da} \left(\sum_{\alpha<\beta} R_{\alpha\beta}^{-1}\right) \\
& + S_{bc}\, S_{cd}(\langle ab|da\rangle - \tfrac{1}{2} S_{ab}\langle a|r_A^{-1}+r_B^{-1}|d\rangle - \tfrac{1}{2} S_{da}\langle a|r_A^{-1}+r_D^{-1}|b\rangle) \\
& + S_{ab}\, S_{bc}(\langle da|cd\rangle - \tfrac{1}{2} S_{da}\langle c|r_A^{-1}+r_D^{-1}|d\rangle - \tfrac{1}{2} S_{cd}\langle a|r_C^{-1}+r_D^{-1}|d\rangle) \\
& + S_{cd}\, S_{da}(\langle bc|ab\rangle - \tfrac{1}{2} S_{bc}\langle a|r_B^{-1}+r_C^{-1}|b\rangle - \tfrac{1}{2} S_{ab}\langle b|r_A^{-1}+r_B^{-1}|c\rangle) \\
& + S_{da}\, S_{ab}(\langle cd|bc\rangle - \tfrac{1}{2} S_{cd}\langle b|r_C^{-1}+r_D^{-1}|c\rangle - \tfrac{1}{2} S_{bc}\langle c|r_B^{-1}+r_C^{-1}|d\rangle) \\
& + S_{ab}\, S_{cd}(\langle ac|db\rangle - \tfrac{1}{2} S_{bc}\langle a|r_B^{-1}+r_C^{-1}|d\rangle - \tfrac{1}{2} S_{da}\langle b|r_A^{-1}+r_D^{-1}|c\rangle) \\
& + S_{bc}\, S_{da}(\langle bd|ac\rangle - \tfrac{1}{2} S_{ab}\langle c|r_A^{-1}+r_B^{-1}|d\rangle - \tfrac{1}{2} S_{cd}\langle a|r_C^{-1}+r_D^{-1}|b\rangle)
\end{aligned} \tag{32}$$

B. Overlap integrals

Explicit expressions for the overlap integrals in Eqs. (4)-(6) can be written as follows:

$$\langle I|I\rangle = 2[2 + 3(S_1^2+S_6^2) - {}^1S - 2^2S + 2(-S_1S_3S_4S_6 - S_1S_2S_5S_6 + 2S_2S_3S_4S_5)] \quad (33)$$

$$\langle II|II\rangle = 2[2 + 3(S_3^2+S_4^2) - {}^1S - 2^2S + 2(-S_1S_3S_4S_6 + 2S_1S_2S_5S_6 - S_2S_3S_4S_5)] \quad (34)$$

$$\langle I|II\rangle = 2[-1 + 3(S_2^2+S_5^2) - {}^1S + {}^2S + 2(2S_1S_3S_4S_6 - S_1S_2S_5S_6 - S_2S_3S_4S_5)] \quad (35)$$

The diatomic overlap integral S_i is defined in Eq. (18) using the subscript notation of Eq. (11).

The term ${}^1S$ is an overlap counterpart to the single exchange term ${}^1J$ defined in Eq. (20) and has the simple form,

$$ {}^1S = \sum_{i=1}^{6} S_i \quad . \quad (36)$$

The term ${}^2S$ is an overlap counterpart to the double exchange term ${}^2J$ defined in Eq. (21) and a grouping of terms similar to that used for ${}^2J$ involving two different permutations of orbitals is also used here:

$$ {}^2S = (S_1S_2S_4 + S_1S_3S_5 + S_2S_3S_6 + S_4S_5S_6) - (S_1^2S_6^2 + S_2^2S_5^2 + S_3^2S_4^2) \ . \quad (37)$$

The overlap counterpart to triple exchange terms are the products of overlap integrals in the right-most parentheses in each of Eqs. (33)-(35).

III. Ab Initio Evaluation of the Surface

The expressions given in the preceding Section for the valence bond formulation are valid for the case where the basis set consists of a single hydrogenic orbital located at each of the four nuclear centers. No approximations have been introduced to simplify or eliminate any integrals that occur. Thus, these expressions yield an ab initio valence bond potential surface when all integrals are evaluated exactly. This task is performed in the present Section and presented for comparison with corresponding results using the method of configuration interaction with the same basis set.

In addition to the singlet valence bond wavefunction, a triplet valence bond wavefunction can be constructed. There are three component structures of the triplet: (i) an AB singlet bond and parallel spin functions on C and D, (ii) an AC singlet bond and parallel spin functions on B and D, and (iii) an AD singlet bond and parallel spin functions on B and C. The mixing of these three structures is determined by solving a set of third-order secular equations.

Several levels of configuration interaction results can be constructed corresponding to various wavefunctions using the four-orbital basis set. In increasing order of accuracy, these are as follows: (i) the molecular orbital, or MO, wavefunction consists of the self-consistent-field matrix Hartree-Fock single determinant, (ii) a two determinant wavefunction, designated C2, consists of an optimal linear combination of the two determinants giving the lowest energy expectation value for $\mathcal{H}$, (iii) the full configuration interaction wavefunction, designated CI, consists of the optimal linear combination of all possible determinants that can be constructed from the basis set. For singlet states, MO, C2 and CI wavefunctions are of interest; for triplet states, only MO and CI wavefunctions are needed.

Calculations are presented in Fig. 1 for the lowest energy singlet and triplet states of square-planar H_4 using the various model wavefunctions. The singlet single-determinant, MO, is not a proper eigenfunction of the D_{4h} symmetry group of the square and is therefore labelled ^1A_g according to the D_{2h} point group. At least two determinants are required in order to obtain a proper symmetry eigenfunction of D_{4h}. However, even with two determinants, the resultant $^1B_{1g}$-C2 energy curve lies above the $^3A_{2g}$-MO curve. The full configuration interaction results, $^1B_{1g}$-CI and $^3A_{2g}$-CI, show the singlet state to be lower in energy over the range of distances shown. The triplet valence bond curve, $^3A_{2g}$-VB, exhibits deviations from the configuration interaction result, but is more similar to $^3A_{2g}$-CI than is the $^3A_{2g}$-MO curve. Finally, the most interesting comparison is between the singlet valence bond and full configuration interaction, $^1B_{1g}$-VB and $^1B_{1g}$-CI, curves. The shapes of the two curves are quite similar, and the minimum energy occurs for both these curves at 2.7 bohr.

Fig. 2 shows the energy of the lowest singlet and triplet states for the various approximate wavefunctions along a linear reaction path passing from the rectangle composed of two H_2 molecules of bond length 1.5 bohr separated by 3.6 bohr going through a square transition state with a side length of 2.7 bohr corresponding to the minimum energy square of Fig. 1. The singlet valence bond and configuration interaction, ^1A_g-VB and ^1A_g-CI, results are in good qualitative agreement along this path and the ordering of singlet and triplet states is also the same for both models. By contrast, the ^1A_g-MO curve becomes quite poor as the system

approaches the square conformation. Not only is there a crossing of the singlet and triplet MO curves, there is also a cusp in the singlet curve at the square transition point. The two-determinant approximation, ^1A_g-C2, eliminates the spurious cusp, but still gives rise to a crossing of the singlet and triplet energy levels.

The purpose of the comparisons in Figs. 1 and 2 is simply to lend some credence to the assertion that the valence bond wavefunction represents a reasonable model for the H_4 system by being in fair agreement with some corresponding configuration interaction results. By continuity, the valence bond model should be expected to provide a reasonable description of the system even in unexplored regions of the surface. Of course, as the basis set is enlarged and improved, various characteristics of the potential surface change[13], e.g. the position and height of the energy minimum in the square-planar H_4 conformation. However, the effects on this comparison of such improvements in the quality of the basis set have not been determined.

IV. Semi-Empirical Approaches

A. London-type potential surface

The most drastic simplification of the energy expression and matrix elements of Eqs. (3)-(9) is achieved with the London approximation,[22] where all diatomic overlap integrals, S_{ab} of Eq. (18), are assumed to be zero. In this case, the energy reduces to the simple form

$$E_{London} = Q - \{\tfrac{1}{2}[(J_1+J_6-J_2-J_5)^2 + (J_2+J_5-J_3-J_4)^2 + (J_3+J_4-J_1-J_6)^2]\}^{\frac{1}{2}}. \quad (38)$$

The diatomic Coulomb and exchange integrals, Q and J_i of Eqs. (10), (12) and (17), are evaluated[23-25] using analytic expressions

$$Q_i = \tfrac{1}{2}[{}^1E_i + {}^3E_i] \quad (39)$$

$$J_i = \tfrac{1}{2}[{}^1E_i - {}^3E_i] \quad (40)$$

where the lowest H_2 singlet and triplet energies, ${}^1E_i$ and ${}^3E_i$, are evaluated from the Morse and anti-Morse functions

$${}^1E_i = D_1 \{\exp[-2\alpha(\Delta R_i)] - 2\exp[-\alpha(\Delta R_i)]\} \quad (41)$$

$${}^3E_i = D_3 \{\exp[-2\beta(\Delta R_i)] + 2\exp[-\beta(\Delta R_i)]\} \quad (42)$$

where

$$\Delta R_i = R_i - R_e. \quad (43)$$

The parameters in Eqs. (41)-(43) are given the values:[25]

$$R_e = 1.40083 \text{ bohr} \quad (44)$$

$$D_1 = 0.174445 \text{ hartree} \quad (45)$$

$$D_3 = 0.072283 \text{ hartree} \quad (46)$$

$$\alpha = 1.04435 \text{ bohr}^{-1} \quad (47)$$

$$\beta = 1.000122 \text{ bohr}^{-1} \quad (48)$$

B. Reduction to a Potential Surface for H_3

If one of the four hydrogen atoms of H_4, center D for instance, is removed to infinity, then each of the three internuclear distances R_{AD}, R_{BD} and R_{CD}, between that atom and the remaining three become infinite. These distances correspond to the numerical indices 3, 5 and 6 in Eq. (11). The consequence is that each of the various Coulomb, exchange and overlap integrals defined in Section IIA and IIB having one of these indices as a subscript has an asymptotic value of zero. The matrix elements of $\mathcal{H}$ in Eqs. (7)-(9) and the overlap integrals in Eqs. (33)-(35) simplify in an obvious manner. A semi-empirical evaluation of the remaining terms has been given previously by Porter and Karplus.[25] The Porter-Karplus approximations are repeated here since they form the major components of the H_4 energy expression and since similar approximations are employed later in the evaluation of the additional terms in the full H_4 energy.

Triatomic integrals Δ_{ab} occur in ${}^1J_1$ of Eq. (15). The expression for Δ_{ab} in Eq. (19) is simplified by using the approximation

$$\langle ac|bc\rangle - \langle a|r_C^{-1}|b\rangle \approx 0 \tag{49}$$

and introducing a multiplicative parameter δ on the remaining terms in Eq. (19). Additional triatomic integrals J_{abc} occur in ${}^2J_{12}$ of Eq. (22). The expression for J_{abc} in Eq. (24) is simplified by using the approximation

$$\langle ac|cb\rangle - \tfrac{1}{2}S_{bc}\langle a|r_B^{-1} + r_C^{-1}|c\rangle - \tfrac{1}{2}S_{ac}\langle b|r_A^{-1} + r_C^{-1}| \rangle \approx 0 \tag{50}$$

and the replacement of reciprocal distances[25] by a parameter ε in Eq. (24)

$$(R_{AB}^{-1} + R_{BC}^{-1} + R_{CA}^{-1}) \approx \varepsilon \ . \tag{51}$$

At first sight, this approximation might appear inappropriate. However, in Eq. (24) ε multiplies a product of three overlap integrals which have exponential R dependencies. At very small R, the approximation of Eq. (51) becomes particularly faulty but this range of R is apparently not of physical importance for trajectory calculations. Further discussion of this approximation has been given.[25]

These approximations and the parameters δ and ε are incorporated into the H_4 surface so that when one atom is removed, the energy reduces to the Porter-Karplus surface for H_3.

C. Parameterization of the H_4 Potential Surface

The expressions in Section IIA and IIB need to be evaluated in order to produce the complete energy expression for H_4.

The diatomic Coulomb, exchange and overlap integrals of Eqs. (12), (17) and (18) are evaluated from the analytic expressions,

$$Q_i - \tfrac{1}{2}[{}^1E_i + {}^3E_i + S_i^2({}^1E_i - {}^3E_i)] \tag{52}$$

$$J_i = \tfrac{1}{2}[{}^1E_i - {}^3E_i + S_i^2({}^1E_i + {}^3E_i)] \tag{53}$$

$$S_i = (1 + \zeta_i R_i + \tfrac{1}{3}\zeta_i^2 R_i^2)\exp(-\zeta_i R_i) \tag{54}$$

where ${}^1E_i$ and ${}^3E_i$ are defined in Eqs. (41)-(48) and

$$\zeta_i = 1 + \kappa \exp(-\lambda R_i) \tag{55}$$

$$\kappa = 0.60 \text{ bohr}^{-1} \tag{56}$$

$$\lambda = 0.65 \text{ bohr}^{-1} . \tag{57}$$

The triatomic term Δ_{ab} of Eq. (19) is simplified[25] by using Eq. (49)

$$\Delta_{ab} \approx \delta S_{ab}^2[R_{AC}^{-1} + R_{BC}^{-1} - \langle c|r_A^{-1} + r_B^{-1}|c\rangle$$

$$+ R_{AD}^{-1} + R_{BD}^{-1} - \langle d|r_A^{-1} + r_B^{-1}|d\rangle] \tag{58}$$

where

$$\langle a|r_B^{-1}|\ a\rangle = R_{AB}^{-1}\,[1 - (1 + R_{AB})\,\exp(-2R_{AB})] \tag{59}$$

and[25]

$$\delta = 1.03640 \text{ hartree} . \tag{60}$$

Additional triatomic integrals J_{abc} and Δ_{abc} occur in ${}^2J_{12}$ of Eq. (22). The expression for J_{abc} in Eq. (24) is simplified[25] by using Eqs. (50)-(51):

$$J_{abc} \approx \varepsilon\, S_{ab}\, S_{bc}\, S_{ca} \tag{61}$$

with[25]

$$\varepsilon = -0.643153 \text{ hartree} . \tag{62}$$

The expression for Δ_{abc} in Eq. (25) is simplified by using Eq. (49):

$$\Delta_{abc} \approx \delta\, S_{ab}\, S_{bc}\, S_{ac}(R_{AD}^{-1} + R_{BD}^{-1} + R_{CD}^{-1} - \langle d|r_A^{-1} + r_B^{-1} + r_C^{-1}|d\rangle\ ) \tag{63}$$

where δ is given above in Eq. (60).

The four-center term $\Delta_{ab,cd}$ of Eq. (28) is simplified by introducing an approximation similar to those of Eqs. (49) and (50):

$$\langle ac|bd\rangle - \tfrac{1}{2}\, S_{cd}\, \langle a|r_C^{-1} + r_D^{-1}|b\rangle - \tfrac{1}{2}\, S_{ab}\, \langle c|r_A^{-1} + r_B^{-1}|\ d\rangle \approx 0 . \tag{64}$$

In the spirit of Eq. (51), the reciprocal distances are replaced by a parameter:

$$\Delta_{ab,cd} \approx \varepsilon_1\, S_{ab}^2\, S_{cd}^2 \tag{65}$$

The remaining four-center term J_{abcd} of Eq. (32) is simplified by using Eqs. (50) and (64) and by replacing reciprocal distances by a parameter:

$$J_{abcd} \approx \varepsilon_2 S_{ab} S_{bc} S_{cd} S_{da}. \tag{66}$$

A problem arises with the approximation for $\Delta_{ab,cd}$ in Eq. (65); namely, with R_{AB} and R_{CD} held constant, and the AC, AD, BC and BD distances increasing, $\Delta_{ab,cd}$ should approach zero, whereas the expression in Eq. (65) is constant. Considerable numerical experimentation with $\Delta_{ab,cd}$ indicated that the dependence on the AC, AD, BC and BD distances should be exponential or at least R^{-6}. These considerations led to the following modification

$$\Delta_{ab,cd} \approx \varepsilon_1 S_{ab}^2 S_{ac} S_{ad} S_{bc} S_{bd} S_{cd}^2 \tag{67}$$

which preserves the form of Eq. (65) while adding overlap factors to enable Δ_{abcd} to approach zero as the AB to CD distance is increased. A slight simplification of Eq. (67) is the following

$$\Delta_{ab,cd} \approx \varepsilon_1 S_{ab} S_{ac} S_{ad} S_{bc} S_{bd} S_{cd} . \tag{68}$$

Table I contains a summary of the parameterization of several H_4 surfaces. All of the Porter-Karplus[25] parameters are employed plus two additional parameters ε_1 and ε_2 to be used in Eqs. (66)-(68). The values of ε_1 and ε_2 for Surfaces A and C were chosen to yield agreement with <u>ab initio</u> configuration interaction calculations[7,13] for a variety of available barrier heights and barrier positions. The values of ε_1 and ε_2 for Surface B where chosen to yield close agreement with an <u>ab initio</u> configuration interaction calculation[10,13] for a linear arrangement of the four atoms.

V. Characteristics of the H_4 Surfaces

The H_4 potential surfaces, A, B, C and D defined in Table I, have been constructed to yield the proper atomic (four H) and diatomic (two H_2) asymptotic limits, each H_2 molecule being described by a Morse potential.[36] With one atom removed, the H_4 surface reduces to the Porter-Karplus[25] potential for three atoms. Contour maps for two geometrical arrangements of the Porter-Karplus H_3 system are given in Fig. 3. It should be noted that, at short internuclear distances there is a peculiar region where the energy becomes sharply negative. Probably, this arises from the use of the approximation in Eq. (51) used to simplify J_{abc} of Eq. (24). This feature apparently does not affect the usefulness of the surface for calculations of H_3 dynamics since a high energy barrier separates it from any reasonable H_3 trajectory.

Although there are six degrees of freedom allowed in the placement of nuclear centers for a four-atom system, planarity and symmetry constraints can be used to reduce this number. Thus the most easily accessible geometrical arrangements are those which maintain the highest symmetries and hence have only one degree of freedon: for instance, the equidistant linear, centered equilateral triangle, tetrahedron, and square configurations. In these cases, it is possible to search for a minimum in the energy with respect to the remaining geometrical parameters. A tabulation of such characteristics is given in Table II. In addition, for several fixed acute angles, the energy of rhombus geometries is given corresponding to a minimum in the energy with respect to the side-length of the rhombus.

The minimum energy for the equidistant linear arrangement is very low (42-56 kcal/mole) relative to the dissociation energy of a single diatomic H_2 (109 kcal/mole) for all four surfaces as well as for various previous

configuration interaction calculations.[7,9,10,13] However, the equidistant linear geometry is not a proper saddle point through which the bimolecular chemical exchange reaction could proceed. Contour maps of the surfaces corresponding to a two-parameter linear conformation are shown in Fig. 4, where the diagonal (x=y) corresponds to the equidistant linear situation. Surface B has a region of spurious negative energy similar to that seen in Fig. 3. Here again, this undesirable feature is separated from the paths of reasonable trajectories by an energy barrier greater than twice the H_2 dissociation energy.

A geometrical arrangement through which chemical exchange is conceivable is the rectangle-square-rectangle shown in Fig. 5. Here both surfaces A and B exhibit the spurious negative feature at short internuclear distances. The saddle-point barrier heights for surfaces A, B and C fall in the range 136-142 kcal/mole which is well above the H_2 dissociation energy. The London surface, D, has a lowest energy square of 73 kcal/mole. Table II shows that as the square is distorted through the rhombus geometry, the lowest saddle point energy for surface D exceeds the H_2 dissociation energy as the acute angle of the rhombus is decreased from 60° to 45°. Surface B has the opposite behavior: as the acute angle decreases, the energy also decreases and drops below the H_2 dissociation energy both at 45° and 30°. These low energies are due to the choice of parameters and functional form used for the various integrals entering the energy expression. Different choices of the parameters (compare surfaces B and C) can increase these low energy barriers as well as change other properties of the surface.

VI. Discussion

Four semi-empirical potential energy surfaces have been developed for the H_4 system. All of them are constructed using the LEPS model.[22-24] One of these, Surface D, incorporates the London approximation[22] where all overlap integrals are taken to be zero. The consequence is that Surface D has very low energy barriers to chemical exchange, especially through the rectangle-square-rectangle geometry. The remaining surfaces, A, B and C, are modelled using the valence bond scheme with an empirical evaluation of three and four center integrals. The three valence bond surfaces incorporate the Porter-Karplus H_3 potential.[25] Thus the asymptotic limit of $H + H_3$ is well known. The molecular limit of $2H_2$ or $H_2 + 2H$ consists of a Morse[36] H_2 molecule. The H atom limit is exact.

The positions and heights of various barriers to chemical exchange on Surfaces A, B and C depend on the parameterization and mathematical form of the approximations for the integrals. In general, the barrier heights are chosen to be high and therefore consistent with <u>ab initio</u> configuration interaction calculations. In addition, these surfaces tend to be steeply repulsive at short internuclear distances.

All four H_4 surfaces are semi-empirical constructions and are therefore not intended to be used to "predict" the existence of possible chemical reaction paths for $H_2 + D_2$ exchange. Instead, the surfaces are intended to mimic previous theoretical results on the H_4 system. Unfortunately, certain discrepancies exist between theoretical[7,13] and experimental[27-31,37] considerations of barrier heights on the H_4 surface. Nevertheless, the surfaces can be used to assess the importance of dynamical effects on chemical reaction and energy exchange processes in four-atom bimolecular collisions.

The four semi-empirical H_4 potential energy surfaces differ from one another in a variety of ways. The effect of these differences on calculations of the dynamics of the bimolecular chemical exchange process is examined in a following paper.[38] Surface D corresponds to the London potential and Surface C is the repulsive model potential: these were used in two previous quasi-classical calculations[39] of reactive and inelastic scattering of $H_2 + D_2$. Surface B has been used[40] in quantum mechanical calculations of vibrational energy exchange during co-linear collisions. Surfaces A and D have been compared with other potentials in quantum mechanical calculations[41] of rotational energy exchange.

References

1. M. Born and J. R. Oppenheimer, Ann. Physik 84, 457 (1927).
2. R. Taylor, Proc. Phys. Soc. (London) A64, 249 (1951).
3. R. S. Barker, R. L. Snow and H. Eyring, J. Chem. Phys. 23, 1686 (1955).
4. V. Magnasco and G. F. Musso, J. Chem. Phys. 46, 4015 (1967); 47, 1723, 4629 (1967); 48, 2657, 2834 (1968); V. Magnasco, G. F. Musso and R. McWeeney, J. Chem. Phys. 47, 4617 (1967).
5. M. E. Schwartz and L. J. Schaad, J. Chem. Phys. 48, 4709 (1968).
6. H. Conroy and G. Malli, J. Chem. Phys. 50, 5049 (1969).
7. M. Rubinstein and I. Shavitt, J. Chem. Phys. 51, 2014 (1969).
8. O. Tapia, G. Bessis and S. Bratož, C. R. Acad. Sci. Paris 268B, 813 (1969); Int. J. Quantum Chem. S4, 289 (1971); O. Tapia, Chem. Phys. Lett. 10, 613 (1971); O. Tapia and G. Bessis, Theoret. Chim. Acta 25, 130 (1972).
9. C. W. Wilson, Jr. and W. A. Goddard III, J. Chem. Phys. 51, 716 (1969); 56, 5913 (1972).
10. C. F. Bender and H. F. Schaefer III, J. Chem. Phys. 57, 217 (1972).
11. C. F. Bender, H. F. Schaefer and P. A. Kollman, Molec. Phys. 24, 235 (1972).
12. E. Kochanski, B. Roos, P. Siegbahn and M. H. Wood, Theoret. Chim. Acta 32, 151 (1973).
13. D. M. Silver and R. M. Stevens, J. Chem. Phys. 59, 3378 (1973).
14. H. Eyring, J. Am. Chem. Soc. 53, 2537 (1931).
15. H. S. W. Massey and R. A. Buckingham, Proc. Roy. Irish Acad. A45, 31 (1938).
16. J. de Boer, Physica 9, 363 (1942).
17. H. Margenau, Phys. Rev. 64, 131 (1943); A. A. Evett and H. Margenau, Phys. Rev. 90, 1021 (1953).

18. V. Griffing, J. Chem. Phys. 23, 1015 (1955); V. Griffing and A. Maček, J. Chem. Phys. 23, 1029 (1955); V. Griffing and J. T. Vanderslice, J. Chem. Phys. 23, 1035 (1955); V. Griffing and J. S. Dooling, J. Phys. Chem. 61, 11 (1957); A. R. Ruffa and V. Griffing, J. Chem. Phys. 36, 1389 (1962).

19. E. A. Mason and J. O. Hirschfelder, J. Chem. Phys. 26, 756 (1957).

20. J. T. Vanderslice and E. A. Mason, J. Chem. Phys. 33, 492 (1960).

21. R. B. Abrams, J. C. Patel and F. O. Ellison, J. Chem. Phys. 49, 450 (1968); B. Freihaut and L. M. Raff, J. Chem. Phys. 58, 1202 (1973).

22. F. London, Z. Elektrochem. 35, 552 (1929).

23. H. Eyring and M. Polanyi, Z. Phys. Chem. Abt. B12, 279 (1931).

24. S. Sato, J. Chem. Phys. 23, 592 (1955); Bull. Chem. Soc. Jpn. 28, 450 (1955).

25. R. N. Porter and M. Karplus, J. Chem. Phys. 40, 1105 (1964).

26. M. Karplus, R. N. Porter and R. D. Sharma, J. Chem. Phys. 43, 3259 (1965); K. T. Tang and M. Karplus, J. Chem. Phys. 49, 1676 (1968); S. Wu and R. D. Levine, Molec. Phys. 22, 881 (1971); D. J. Diestler, J. Chem. Phys. 54, 4547 (1971); G. Wolken Jr., W. H. Miller and M. Karplus, J. Chem. Phys. 56, 4930 (1972).

27. S. H. Bauer and E. Ossa, J. Chem. Phys. 45, 434 (1966); A. Burcat and A. Lifshitz, J. Chem. Phys. 47, 3079 (1967); D. Lewis and S. H. Bauer, J. Am. Chem. Soc. 90, 5390 (1968).

28. R. D. Kern and G. G. Nika, J. Phys. Chem. 75, 1615, 2541 (1971).

29. L. L. Poulsen, J. Chem. Phys. 53, 1987 (1970).

30. S. H. Bauer, D. M. Lederman, E. L. Resler, Jr. and E. R. Fisher, Int. J. Chem. Kinetics 5, 93 (1973).

31. F. Kaufman, Ann. Rev. Phys. Chem. 20, 62 (1969).

32. R. Hoffmann, J. Chem. Phys. 49, 3739 (1968); D. M. Silver, Chem. Phys. Lett. 14, 105 (1972).

33. A. K. McMahan, H. Beck and J. A. Krumhansl, Phys. Rev. A 9, 1852 (1974).

34. R. Gegenbach, C. Hahn, W. Schrader and J. P. Toennies, Theoret. Chim. Acta 34, 199 (1974).

35. J. C. Slater, Phys. Rev. 38, 1109 (1931).

36. P. M. Morse, Phys. Rev. 34, 57 (1929).

37. A. Lifshitz and M. Frenlach, J. Chem. Phys. 67, 2803 (1977).

38. N. J. Brown and D. M. Silver, J. Chem. Phys. (following paper).

39. N. J. Brown and D. M. Silver, J. Chem. Phys. 65, 311 (1976); 68, 3607 (1978).

40. M. H. Alexander, J. Chem. Phys. 59, 6254 (1973); 60, 4274 (1974).

41. R. Ramaswamy, H. Rabitz and S. Green, J. Chem. Phys. 66, 3021 (1977).

Table I. Definition of parameters for the H_4 surfaces[a]

Surface	type	$\Delta_{ab,cd}$	ε_1	ε_2
A	valence bond	Eq. (68)	20.7	-1.4
B	valence bond	Eq. (67)	27.0	-1.95
C	valence bond	Eq. (67)	140.0	-0.97
D	London	—	—	—

[a] ε_1 and ε_2 are given in hartrees, see Eqs. (66)-(68).

Table II. Characteristics of various H_4 surfaces

Surface	R_{min} (bohr)	$E_{min}(H_4)$ (hartree)	$E(2H_2)$ (hartree)	ΔE(barrier) (kcal/mole)
Equidistant linear				
A	1.68	-2 2821	-2.3489	42
B	1.69	-2.2775	-2.3489	45
C	1.80	-2.2710	-2.3489	49
D	1.72	-2.2597	-2.3489	56
CI(WG)[a]	1.8	-2.2108	-2.2959	53
CI(RS)[b]	1.7	-2.234	-2.302	43
CI(SS)[c]	1.8	-2.2355	-2.3035	43
CI(BS)[d]	1.67	-2.2615	-2.3314	44
Centered equilateral triangle				
A	2.10	-2.0858	-2.3489	165
B	1.95	-2.1049	-2.3489	153
C	2.31	-2.0767	-2.3489	171
D	2.02	-2.0812	-2.3489	168
CI(SS)[c]	2.2	-2.0448	-2.3035	162
Tetrahedron				
A	2.87	-2.0541	-2.3489	185
B	2.63	-2.0753	-2.3489	172
C	3.20	-2.0448	-2.3489	191
D	2.25	-2.1172	-2.3489	145
CI(RS)[b]	3.8	-2.002	-2.302	188
Square (90° rhombus)				
A	2.42	-2.1322	-2.3489	136
B	2.40	-2.1284	-2.3489	138
C	2.67	-2.1223	-2.3489	142
D	1.94	-2.2321	-2.3489	73
VB(single-zeta)	2.70	-2.0543	-2.2947	151
CI(single-zeta)	2.70	-2.0595	-2.2959	148
CI(WG)[a]	2.75	-2.0587	-2.2959	149
CI(RS)[b]	2.47	-2.075	-2.302	142
CI(SS)[c]	2.44	-2.0785	-2.3053	142

Table II (continued)

Surface	R_{min} (bohr)	$E_{min}(H_4)$ (hartree)	$E(2H_2)$ (hartree)	ΔE(barrier) (kcal/mole)
60° rhombus				
A	2.48	-2.1077	-2.3489	151
B	2.13	-2.1411	-2.3489	130
C	2.73	-2.0999	-2.3489	156
D	2.02	-2.1883	-2.3489	101
CI(SS)[c]	2.20	-2.0724	-2.3035	145
45° rhombus				
A	2.38	-2.1191	-2.3489	144
B	2.18	-2.1792	-2.3489	107
C	2.82	-2.0849	-2.3489	166
D	2.17	-2.1158	-2.3489	146
30° rhombus				
A	2.73	-2.1621	-2.3489	117
B	2.42	-2.1884	-2.3489	101
C	2.99	-2.1517	-2.3489	124
D	3.18	-2.1388	-2.3489	132

[a]Ref. 9
[b]Ref. 7
[c]Ref. 13
[d]Ref. 10

FIGURE CAPTIONS

Figure 1. Potential energy curves representing the lowest singlet and triplet states of square-planar H_4 with CI, VB, MO and C_2 wave functions.

Figure 2. Potential energy curves representing the lowest singlet and triplet states along a linear quasi-reaction path of rectangular $2H_2$ going through square H_4 with CI, VB, MO and C_2 wave functions.

Figure 3. Equipotential contour maps for the Porter-Karplus H_3 surface corresponding to linear and triangular arrangements of the three atoms. The contour intervals are 1/10 of the H_2 dissociation energy. The hatched regions are spurious properties of the potential surfaces.

Figure 4. Equipotential contour maps for the H_4 surfaces corresponding to linear arrangements of the four atoms. The contour intervals are 1/10 of the H_2 dissociation energy. The hatched regions are spurious properties of the potential surfaces.

Figure 5. Equipotential contour maps for the H_4 surfaces corresponding to rectangular arrangements of the four atoms. The contour intervals are 1/10 of the H_2 dissociation energy. The hatched regions are spurious properties of the potential surfaces.

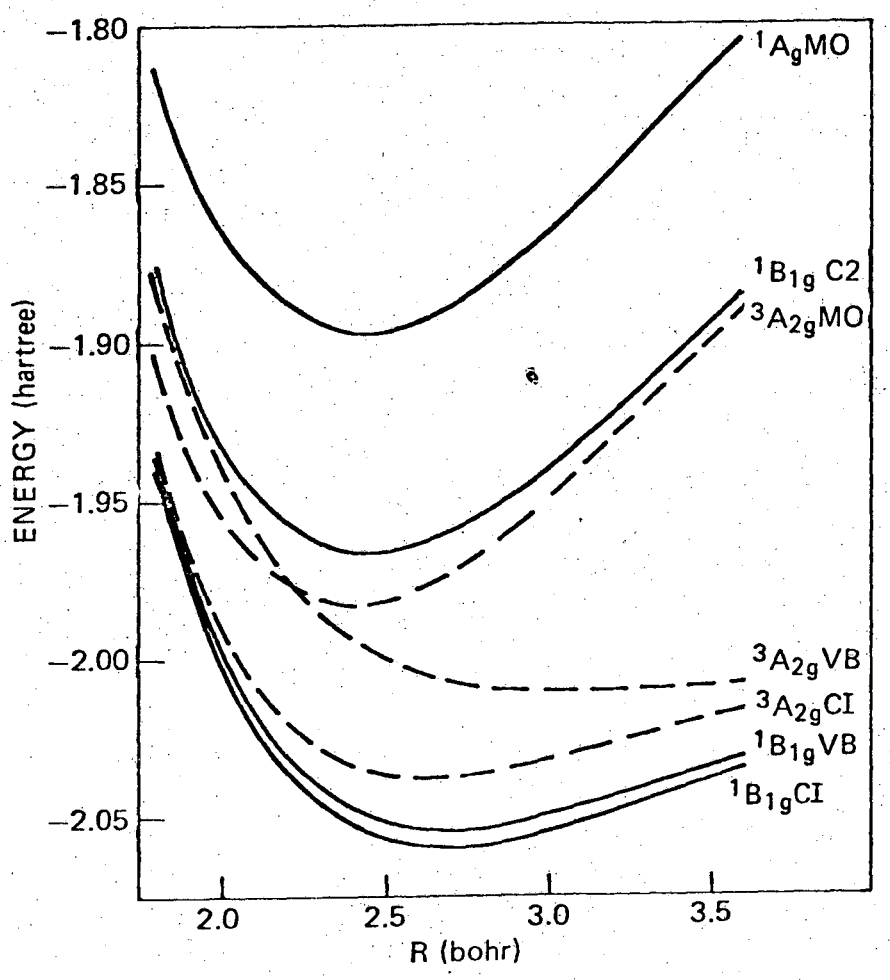

Figure 1. Potential energy curves representing the lowest singlet and triplet states of square-planar H_4 with CI, VB, MO and C_2 wave functions.

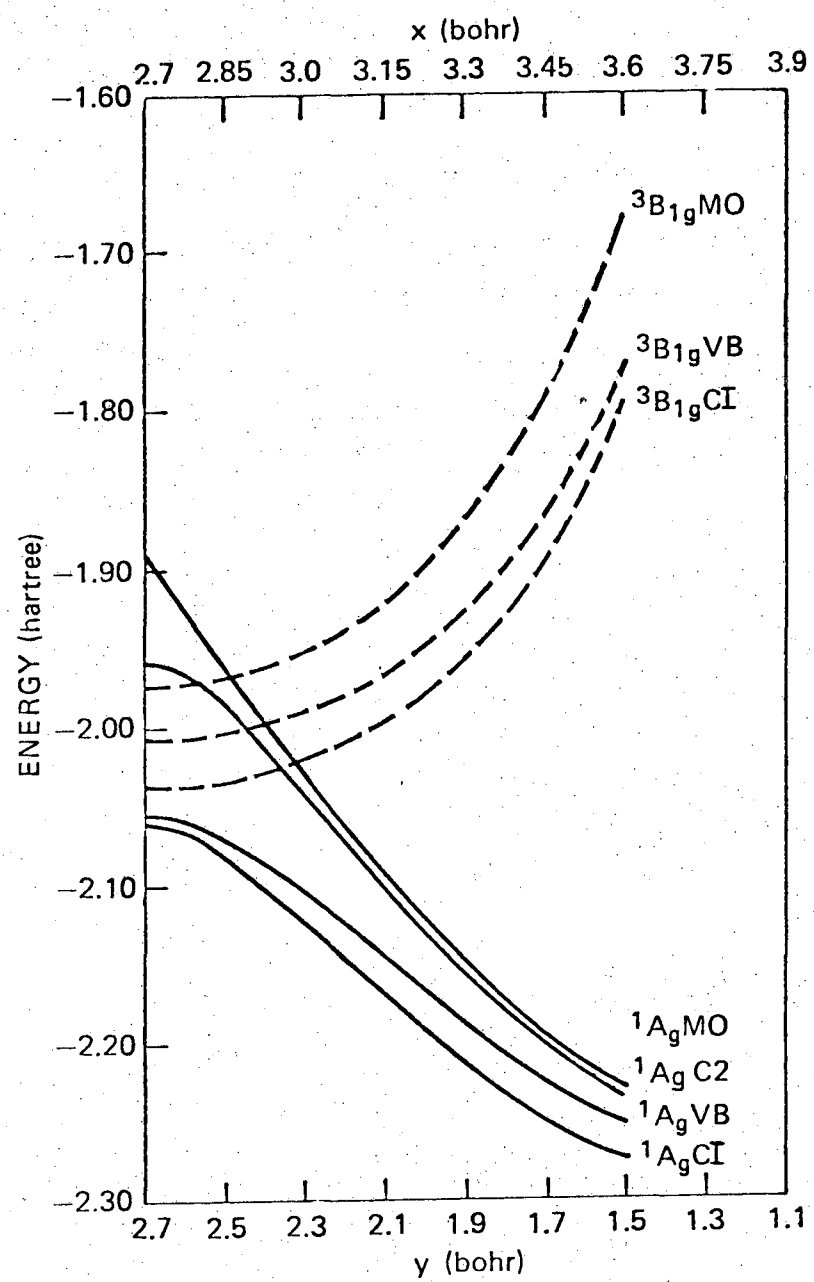

Figure 2. Potential energy curves representing the lowest singlet and triplet states along a linear quasi-reaction path of rectangular $2H_2$ going through square H_4 with CI, VB, MO and C_2 wave functions.

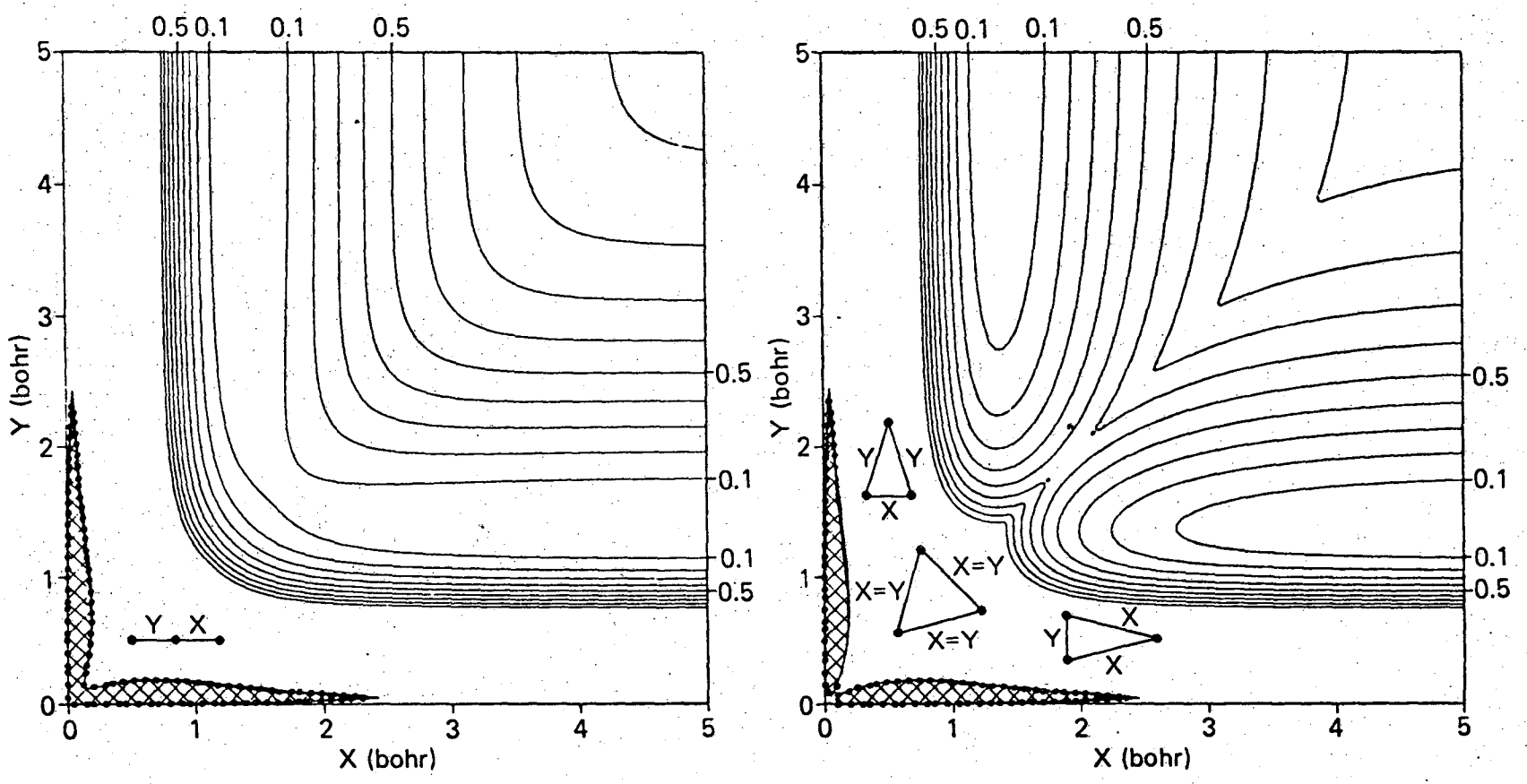

Figure 3. Equipotential contour maps for the Porter-Karplus H_3 surface corresponding to linear and triangular arrangements of the three atoms. The contour intervals are 1/10 of the H_2 dissociation energy. The hatched regions are spurious properties of the potential surfaces.

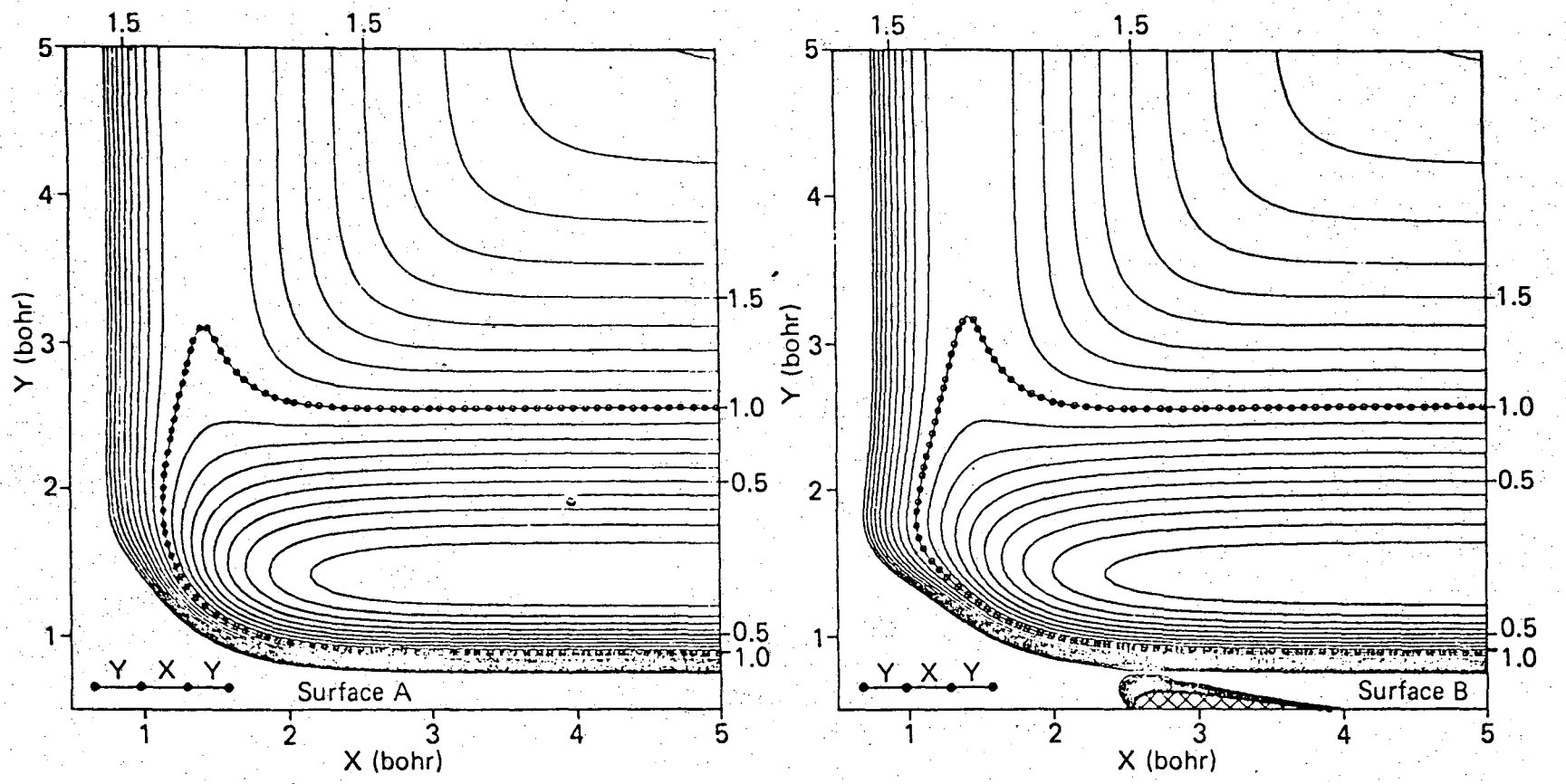

Figure 4a. Equipotential contour maps for the H_4 surfaces corresponding to linear arrangements of the four atoms. The contour intervals are 1/10 of the H_2 dissociation energy. The hatched regions are spurious properties of the potential surfaces.

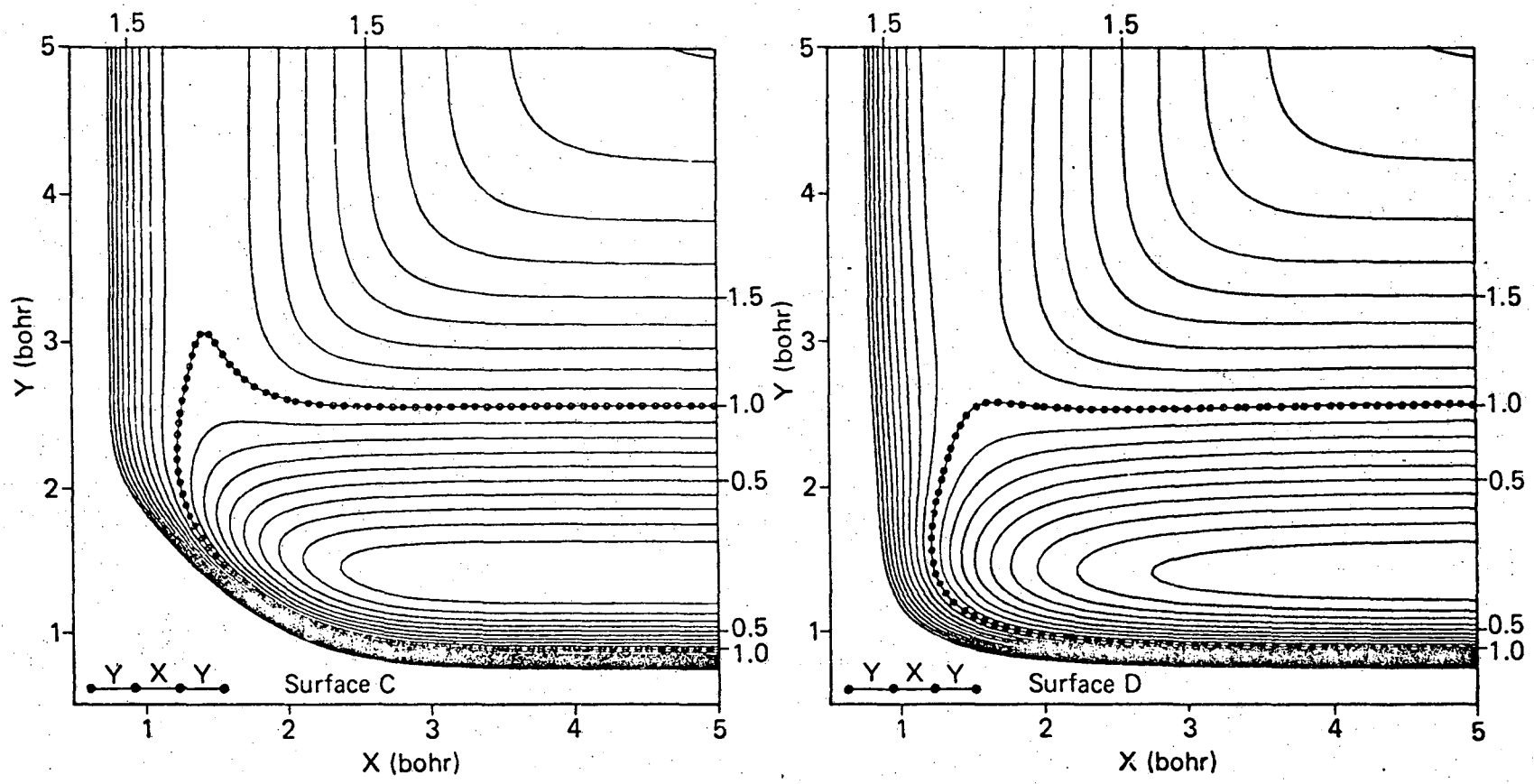

Figure 4b. Equipotential contour maps for the H_4 surfaces corresponding to linear arrangements of the four atoms. The contour intervals are 1/10 of the H_2 dissociation energy. The hatched regions are spurious properties of the potential surfaces.

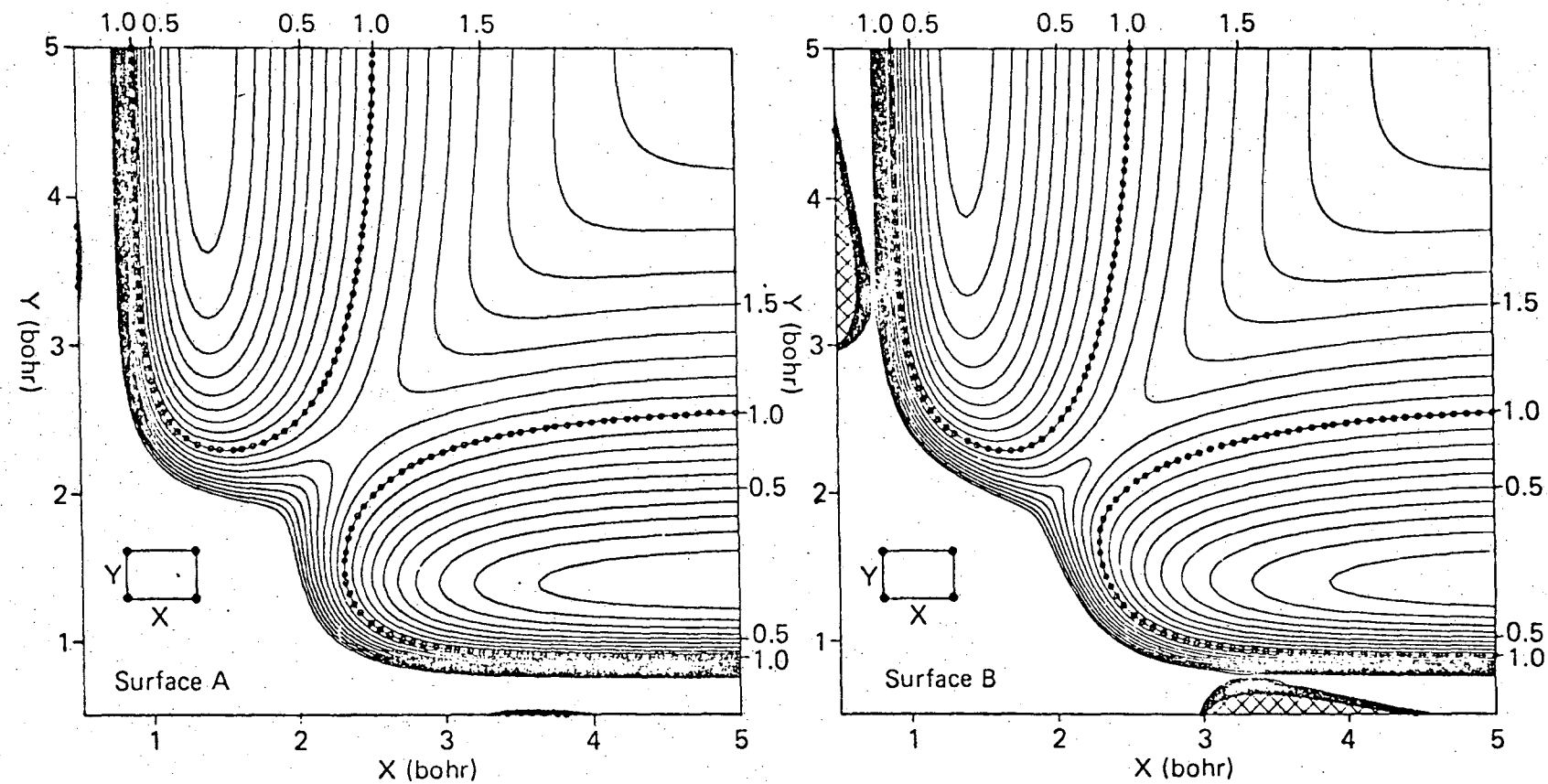

Figure 5a. Equipotential contour maps for the H_4 surfaces corresponding to rectangular arrangements of the four atoms. The contour intervals are 1/10 of the H_2 dissociation energy. The hatched regions are spurious properties of the potential surfaces.

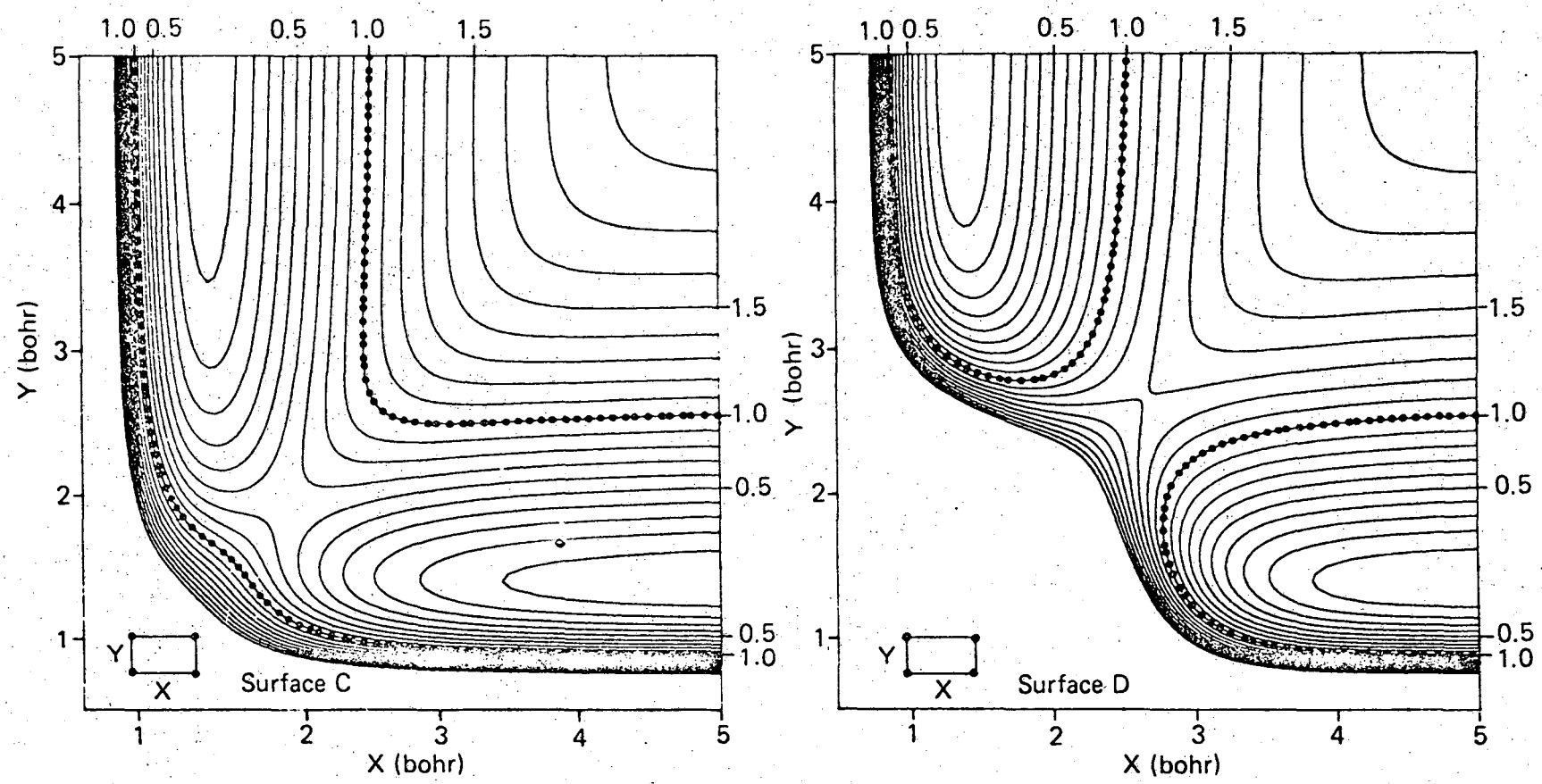

Figure 5b. Equipotential contour maps for the H_4 surfaces corresponding to rectangular arrangements of the four atoms. The contour intervals are 1/10 of the H_2 dissociation energy. The hatched regions are spurious properties of the potential surfaces.

This report was done with support from the Department of Energy. Any conclusions or opinions expressed in this report represent solely those of the author(s) and not necessarily those of The Regents of the University of California, the Lawrence Berkeley Laboratory or the Department of Energy.

Reference to a company or product name does not imply approval or recommendation of the product by the University of California or the U.S. Department of Energy to the exclusion of others that may be suitable.

TECHNICAL INFORMATION DEPARTMENT
LAWRENCE BERKELEY LABORATORY
UNIVERSITY OF CALIFORNIA
BERKELEY, CALIFORNIA 94720